Imperial College London

EE4-13 Adaptive Signal Processing and Machine Intelligence (2018-2019)

Imperial College London

Department of Electrical and Electronic Engineering

Coursework

Authors: CID

Adel Haddad 01060023

Supervisor:

Prof. Danilo P. Mandic

Date: April 2019

Word Count: 0

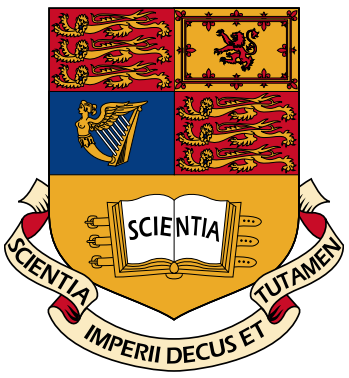

Contents

Contents **1**

1 Classical and Modern Spectrum Estimation **2**
1.1 Properties of Power Spectral Density (PSD) . . . 2
1.1.a Approximation in the Definition of PSD . . . 2
1.1.b Simulation of the Limiting Case . . . 2
1.2 Periodogram-based Methods Applied to Real–World Data . . . 2
1.2.a The SunSpot Dataset . . . 2
1.2.b The EEG Dataset . . . 3
1.3 Correlation Estimation . . . 4
1.3.a Unbiased and Biased ACF Estimates . . . 4
1.3.b Biased ACF Estimator PSDs . . . 4
1.3.c Biased ACF Estimator PSDs on the dB Scale . . . 5
1.3.d Influence of Data Samples on the PSD . . . 5
1.3.e MUltiple SIgnal Classification (MUSIC) Estimator . . . 6
1.4 Spectrum of Autoregressive (AR) Processes . . . 6
1.4.a Shortcomings of the Unbiased ACF in finding AR Parameters . . . 6
1.4.b Error of the AR PSD Estimate . . . 7
1.4.c Error of the AR PSD Estimate with more Samples . . . 7
1.5 Real World Signals: Respiratory Sinus Arrhythmia from RR-Intervals . . . 8
1.5.a Standard & Average PSDs of the RRI Dataset . . . 8
1.5.b Analysis of the RRI PSD Estimates . . . 8
1.5.c AR PSD Estimate for the RRI Dataset . . . 9
1.6 Robust Regression . . . 10
1.6.a Single Value Decomposition (SVD) . . . 10
1.6.b Low Rank Approximation Error . . . 10
1.6.c Ordinary Least Squares (OLS) & Principle Component Regression (PCR) Estimate Errors . . . 10
1.6.d Ordinary Least Squares (OLS) & Principle Component Regression (PCR) Estimate Errors - Part 2 . . . 11

1 Classical and Modern Spectrum Estimation

1.1 Properties of Power Spectral Density (PSD)

1.1.a Approximation in the Definition of PSD

Starting with the equation provided, (1), we: use the relationship between modulus and complex conjugate for complex numbers, we move out the summation terms from the expectation operator, we factor out the exponential terms - as they are independent of the random variable x and we finally use the property that the expectation of a complex conjugate is .....

$$
\begin{aligned}
P(\omega) &= \lim_{N\to\infty} \mathbb{E}\left\{\frac{1}{N}\left|\sum_{n=0}^{N-1} x(n)e^{-j\omega n}\right|^2\right\} \qquad (1)\\
&= \lim_{N\to\infty} \mathbb{E}\left\{\frac{1}{N}\sum_{m=0}^{N-1} x(m)e^{-j\omega m}\sum_{k=0}^{N-1} x^*(k)e^{j\omega k}\right\}\\
&= \lim_{N\to\infty} \frac{1}{N}\sum_{m=0}^{N-1}\sum_{k=0}^{N-1} \mathbb{E}\left\{x(m)e^{-j\omega m}x^*(k)e^{j\omega k}\right\}\\
&= \lim_{N\to\infty} \frac{1}{N}\sum_{m=0}^{N-1}\sum_{k=0}^{N-1} \mathbb{E}\left\{x(m)x^*(k)\right\}e^{-j\omega(m-k)}\\
&= \lim_{N\to\infty} \frac{1}{N}\sum_{m=0}^{N-1}\sum_{k=0}^{N-1} r_{xx}(m-k)e^{-j\omega(m-k)} = \lim_{N\to\infty} \frac{1}{N}\sum_{m=0}^{N-1}\sum_{k=0}^{N-1} g(m-k) \qquad (2)
\end{aligned}
$$

where $g(\tau) = r_{xx}(\tau)e^{-j\omega\tau}$

We can convert the double summation into a single summation using:

$$
\sum_{m=-N}^{N}\sum_{k=-N}^{N} g(m-k) = \sum_{\tau=-2N}^{2N}(2N+1-|\tau|)g(\tau) \qquad (3)
$$

(2) can then be written as:

$$
\begin{aligned}
P(\omega) &= \lim_{N\to\infty}\frac{1}{N}\sum_{\tau=-(N-1)}^{N-1}(N-|\tau|)r_{xx}(\tau)e^{-j\omega\tau}\\
&= \lim_{N\to\infty}\sum_{\tau=-(N-1)}^{N-1} r_{xx}(\tau)e^{-j\omega\tau} - \lim_{N\to\infty}\frac{1}{N}|\tau|\sum_{\tau=-(N-1)}^{N-1} r_{xx}(\tau)e^{-j\omega\tau}\\
&\approx \sum_{\tau=-\infty}^{\infty} r_{xx}(\tau)e^{-j\omega\tau} \qquad (4)
\end{aligned}
$$

1.1.b Simulation of the Limiting Case

1.2 Periodogram-based Methods Applied to Real–World Data

1.2.a The SunSpot Dataset

The mean's influence on data is the offset DC bias, captured in the $f = 0$ component of the periodogram. Hence as we would expect, subtracting the `mean` reduces its magnitude in the periodogram. `detrend` removes linear trends, it seems in the case of this data set that most linear trends are captured at $f \lessapprox 0.02 rad/sample$.

The natural logarithm was taken using: `log`. As the logarithm has a compression effect on magnitude we see that the magnitude of both raw and periodogram is greatly attenuated. We note that frequencies of interest and its harmonics appear as more distinct when compared to the rest of the periodogram.

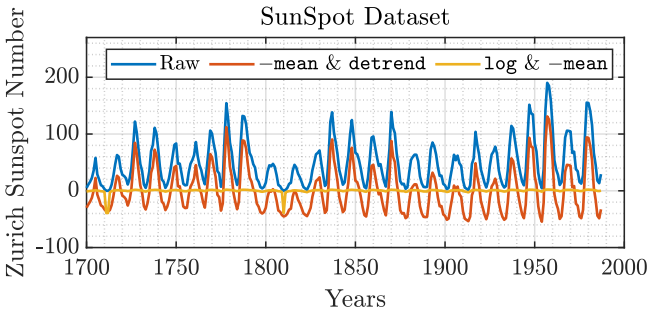

(a) Raw and its preprocessed datas

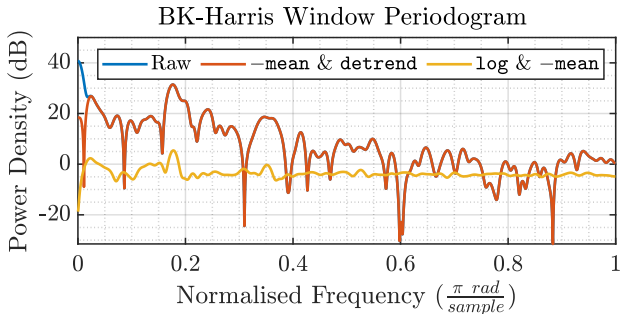

(b) Periodograms

Figure 1.2.1

1.2.b The EEG Dataset

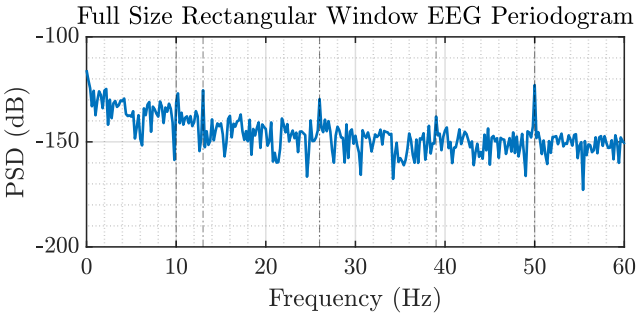

(a) Standard Periodogram

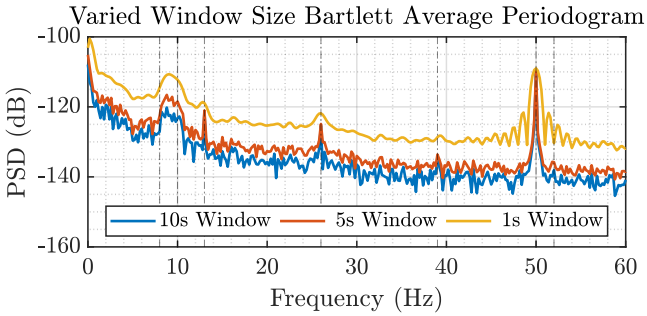

(b) Bartlett Average Periodograms

Figure 1.2.2

Response	**Expected Range** (Hz)	**Observed Range** (Hz)
Alpha Rhythm	$8-10$	$8-10$
SSVEP	`range`$[11-20]$	$13n$
Power-Line	50	50

Table 1.2.1: EEG Frequency Peaks of the Periodogram. n refers to harmonics

The standard periodogram has identifiable peaks - except for the 3rd harmonic of the SSVEP, at 52Hzs it is too close to the power-line interference at 50Hz. The main difference in the 10s window averaged periodogram is clearer peak isolation compared to the surrounding periodogram and emphasis on the range of frequencies of the alpha-rhythm, rather than a single discrete peak.

1.3 Correlation Estimation

1.3.a Unbiased and Biased ACF Estimates

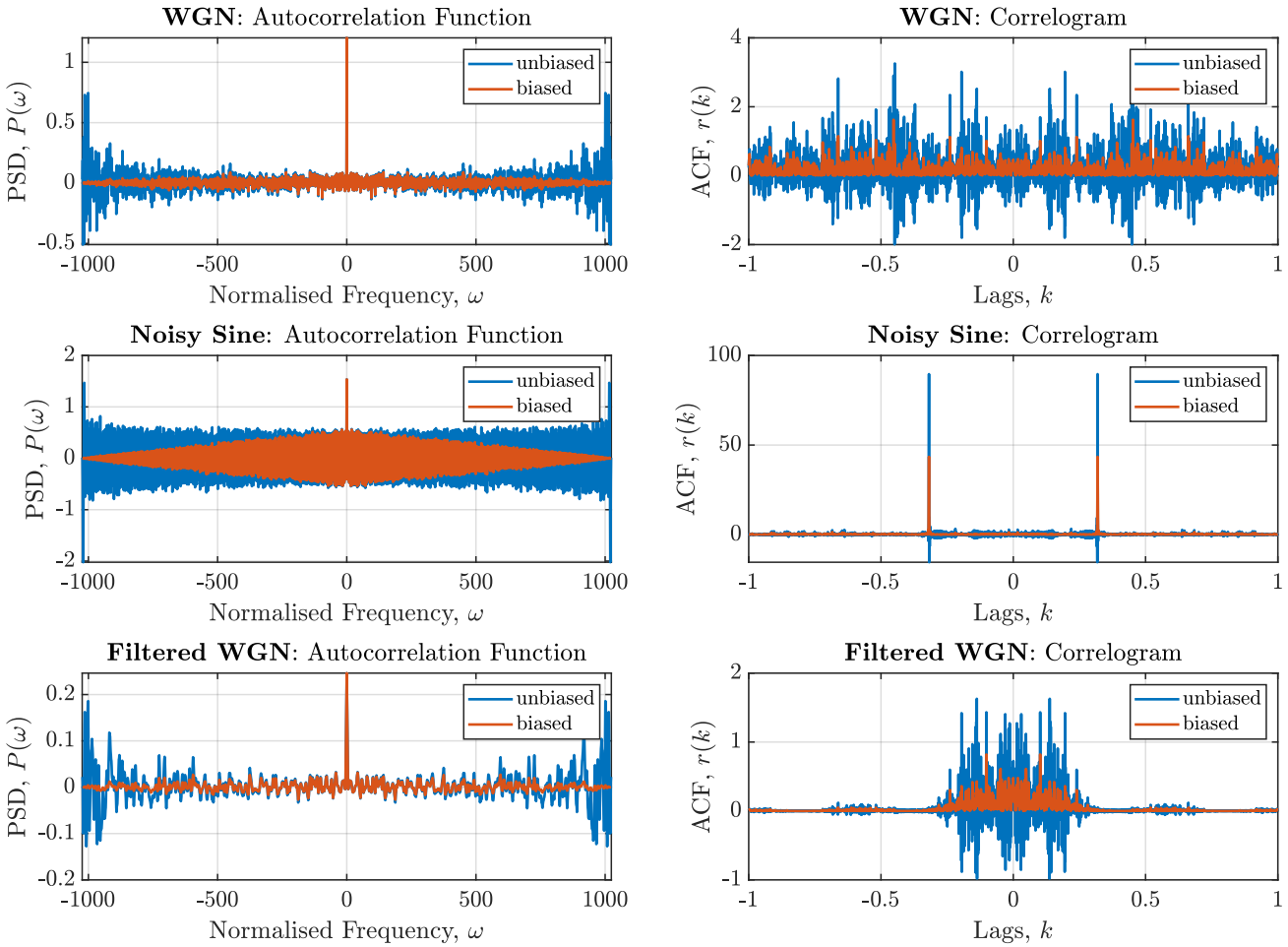

Figure 1.3.1: Set of Auto-Correlation Functions (ACFs) and their Correlograms

For the autocorrelation functions: we can see that the biased estimator tends to 0 for increasing lag magnitude, whereas the unbiased estimator remains somewhat constant, although at the extremes it begins to increase to approximately double the constant value.
For the correlograms: we observe that the biased estimator does not contain negative values.

1.3.b Biased ACF Estimator PSDs

The process simulated was the following:

$$x(n) = 2sin(2\pi 0.4n) + 1.75sin(2\pi 0.6n) + 0.85sin(2\pi 0.85n) + 1.2sin(2\pi 0.95n) + \eta(n) \quad \eta \sim \mathcal{N}(0,1) \tag{5}$$

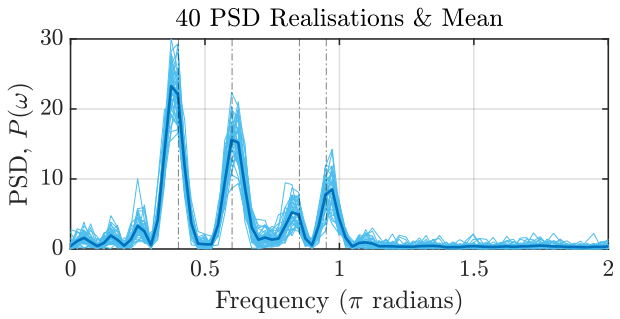

(a) Periodogram

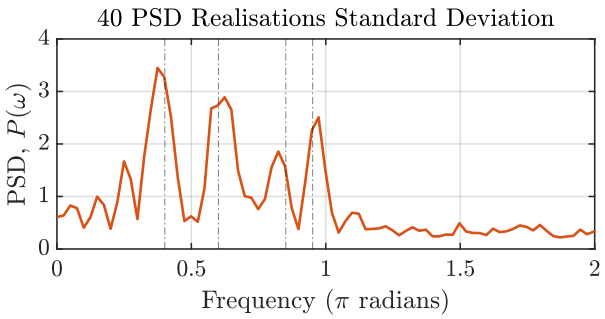

(b) Standard Deviation

Figure 1.3.2: The total number of data points used was 512, black vertical lines indicate the model defined frequencies

It is interesting to see the low frequency resolution influences the accuracy of the peak with respect to the actual frequencies used.

1.3.c Biased ACF Estimator PSDs on the dB Scale

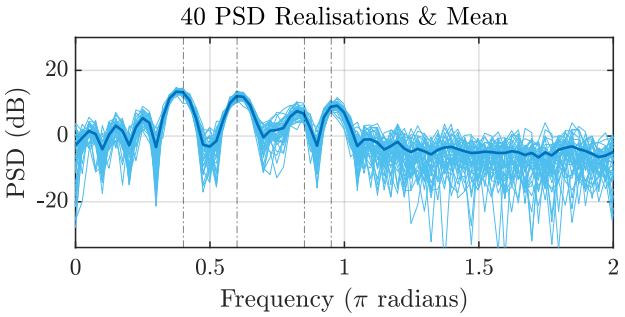

(a) Periodogram

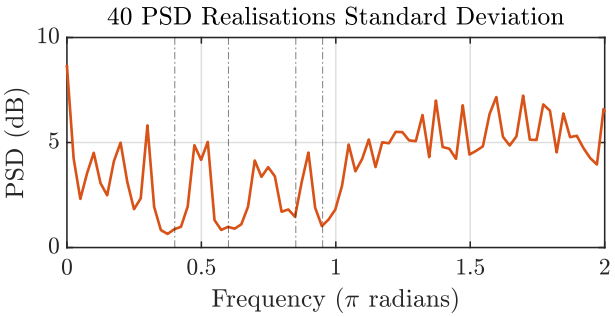

(b) Standard Deviation

Figure 1.3.3: The total number of data points used was 512, black vertical lines indicate the model defined frequencies

It is advantageous that the standard deviation decreases around our frequencies of interest instead of increase.

1.3.d Influence of Data Samples on the PSD

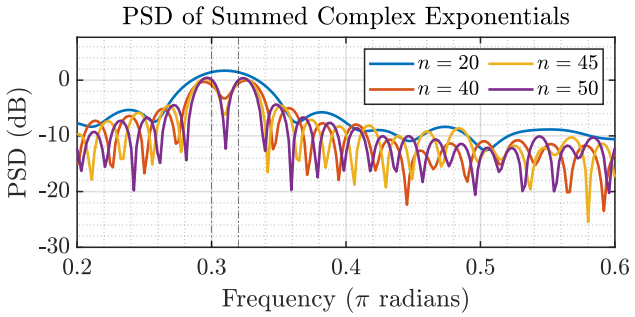

Figure 1.3.4: PSD while varying n, the number of Data Samples used

Here we can clearly see that the frequency resolution is insufficient at lower sample numbers, resulting in aliasing of the desired frequency peaks.

1.3.e MUltiple SIgnal Classification (MUSIC) Estimator

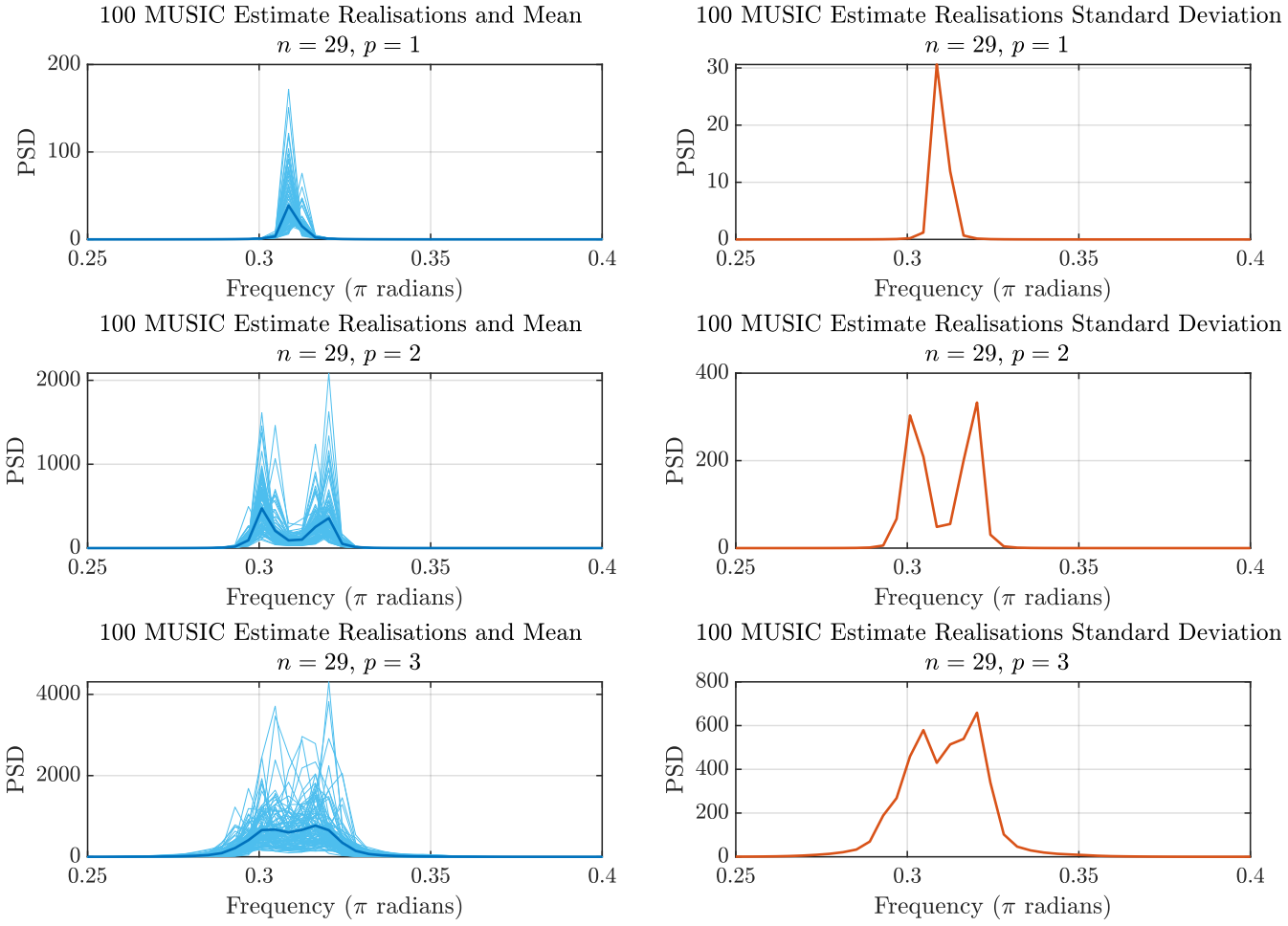

Figure 1.3.5: Set of Auto-Correlation Functions (ACFs) and their Correlograms.
n is the number of samples used, p is the Signal Space Dimensionality

1.4 Spectrum of Autoregressive (AR) Processes

1.4.a Shortcomings of the Unbiased ACF in finding AR Parameters

As the unbiased estimator allows for negative values, at a computational level it will require more bits to store, especially for larger values.

1.4.b Error of the AR PSD Estimate

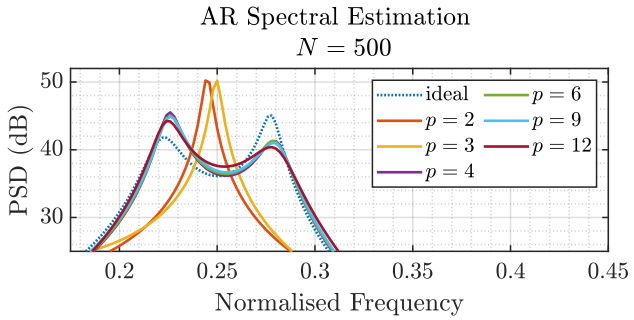

(a) AR Periodogram and its p Order Estimates

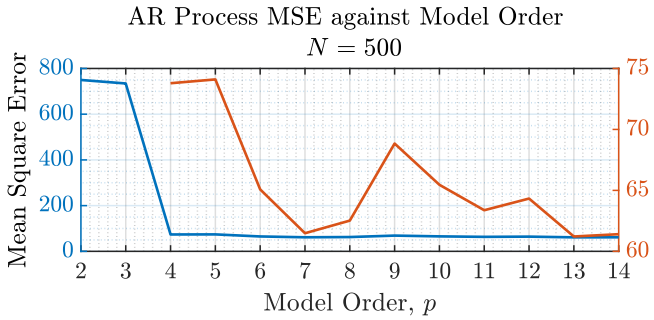

(b) Mean Squared Error

Figure 1.4.1

We can see in (a) of 1.4.1, that increasing the order tends towards a better solution. But (b) notes that the most drastic difference is at the model order, 4, which matches the order of the process defined, subsequent increases of the model order do increase its likeliness to the true response, but changes are not so drastic.

1.4.c Error of the AR PSD Estimate with more Samples

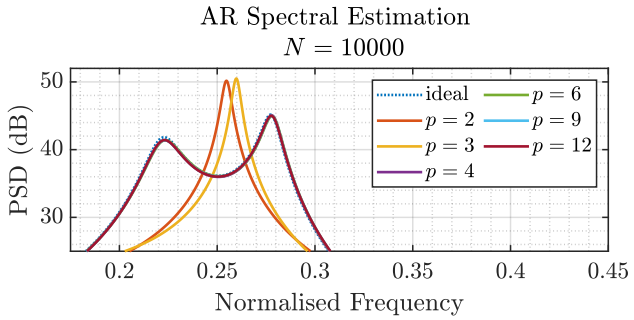

(a) AR Periodogram and its p Order Estimates

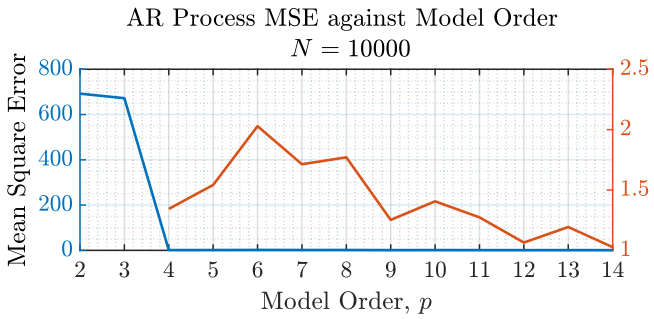

(b) Mean Squared Error

Figure 1.4.2

The same trend is observed as we was with $N = 500$, although the estimate now matches the underlying model much better, reflected in the drastically lower MSE.

It is noted that for a more valid comparison of model order's influence on the estimate's error the Akaike Information Criterion (AIC) or the Bayesian Information Criterion (BIC) are more suitable quantifiers than MSE. But the trend reflected in MSE is still valid.

1.5 Real World Signals: Respiratory Sinus Arrhythmia from RR-Intervals

1.5.a Standard & Average PSDs of the RRI Dataset

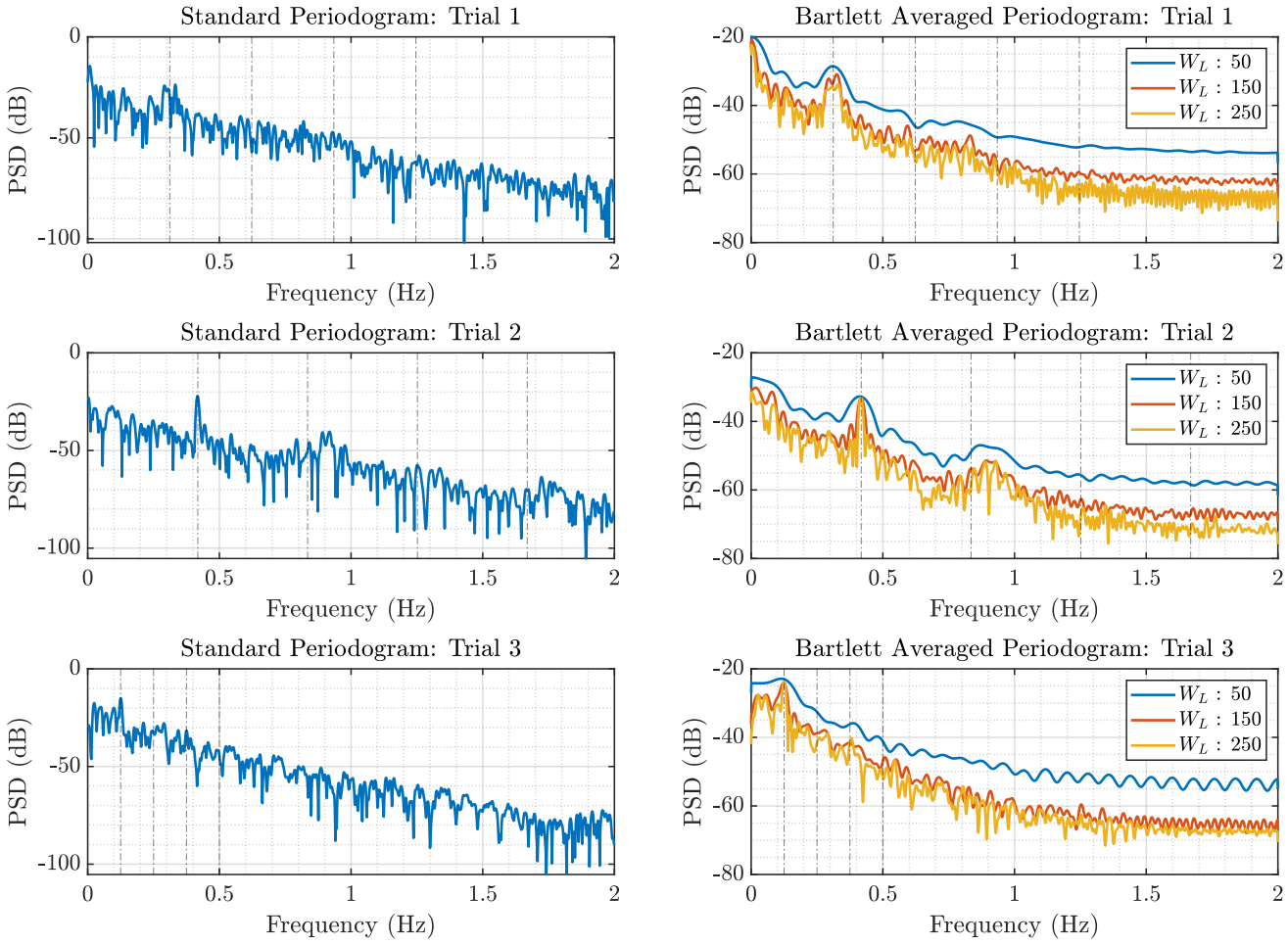

Figure 1.5.1: Standard and Bartlett Average Periodograms.
W_L is the Window Length used

Breathing Type	**Expected** (BPM)	**Observed Peak** (BPM)
Normal (Trial 1)	$10 - 15$	$0.31 \times 60 \approx 18.7$
Fast (Trial 2)	25	$0.41 \times 60 \approx 25$
Slow (Trial 3)	7.5	$0.125 \times 60 = 7.5$

Table 1.5.1: Breaths Per Minute (BPM), i.e. Observed Frequency $\times 60$, for all trials. First 4 harmonics denoted by vertical black lines. Zero Padded Signal Length: 4096

1.5.b Analysis of the RRI PSD Estimates

We can observe distinct peaks for each trial that somewhat agrees with the breathing expected. We note that harmonics are difficult to distinguish, despite the large zero padding of the signal.

1.5.c AR PSD Estimate for the RRI Dataset

The AR spectral estimate correctly identified the peak from models of order $p \gtrapprox 10$. We note that the estimate resembles a smooth envelope over our PSD and correctly identifies clear peaks in the standard PSD at $p = 10$. We also can see for higher order models that there are move fluctuations as the model starts to overfit for the input data's natural noisiness.

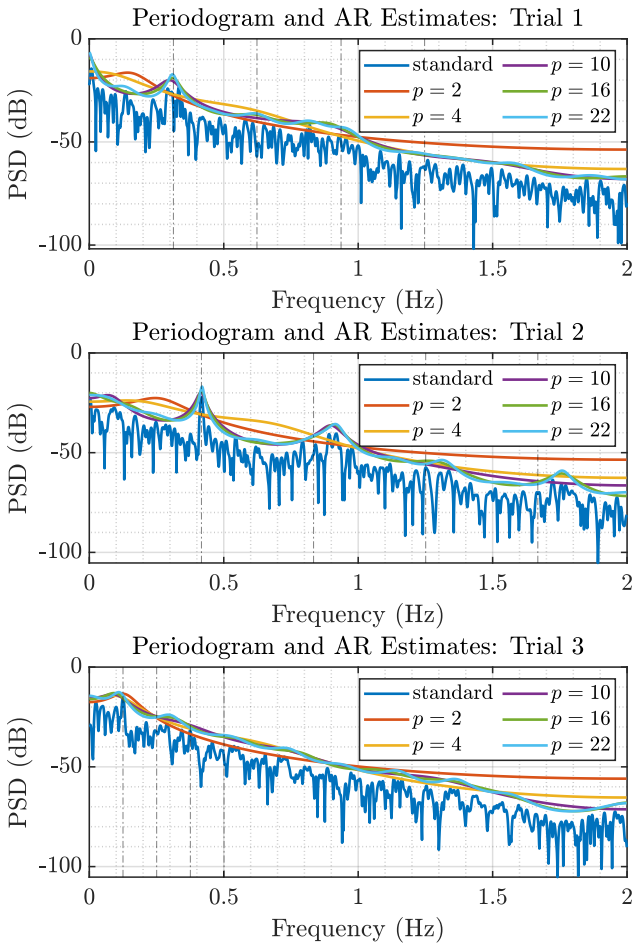

Figure 1.5.2: AR Estimate Periodograms. p is the model order.

1.6 Robust Regression

1.6.a Single Value Decomposition (SVD)

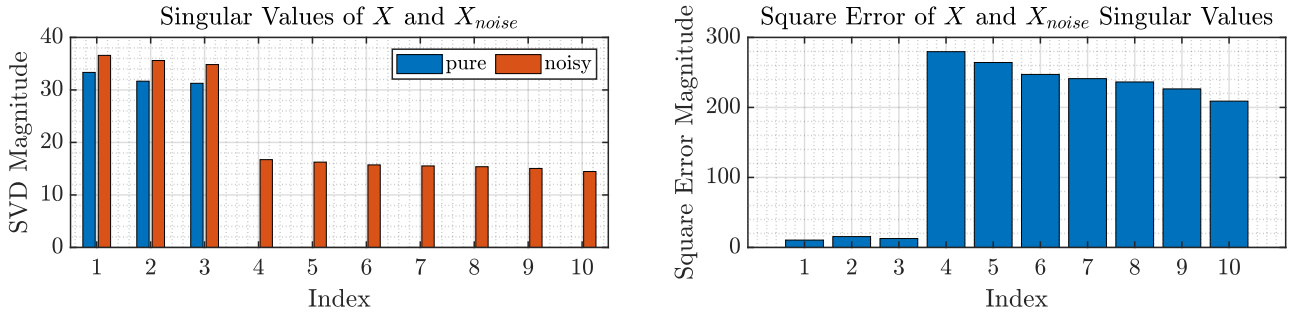

(a) SVD

(b) Square Error

Figure 1.6.1

1.6.b Low Rank Approximation Error

Text here

1.6.c Ordinary Least Squares (OLS) & Principle Component Regression (PCR) Estimate Errors

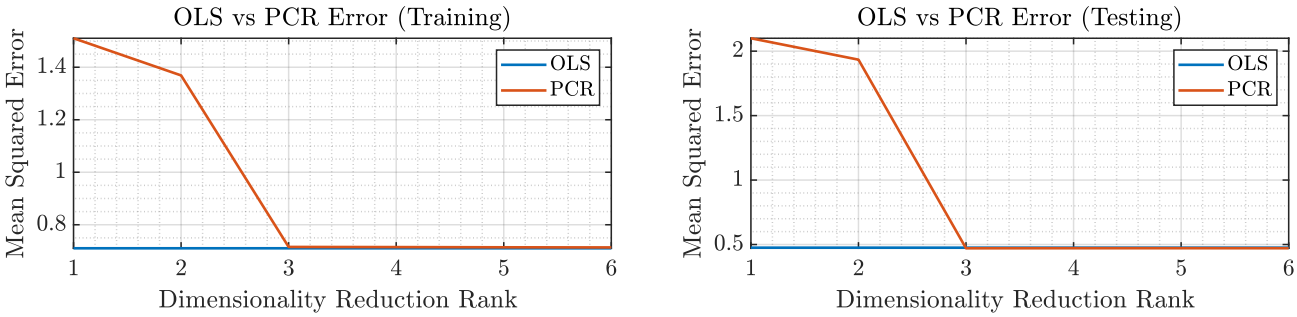

(a) Training Dataset Error

(b) Testing Dataset Error

Figure 1.6.3

1.6.d Ordinary Least Squares (OLS) & Principle Component Regression (PCR) Estimate Errors - Part 2

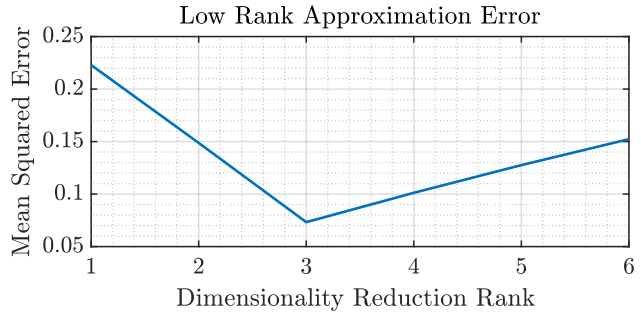

Figure 1.6.2: Effect of Changing Rank on the Approximation Error

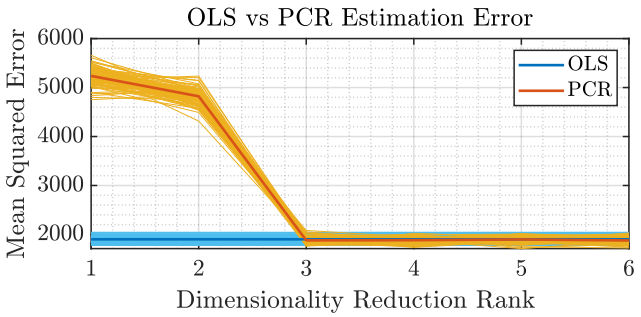

Figure 1.6.4: Mean Sqaure Error over several Realisations